

Task-centric Optimization of Configurations for Assistive Robots

Ariel Kapusta · Charles C. Kemp

Received: date / Accepted: date

Abstract Robots can provide assistance to a human by moving objects to locations around the person’s body. With a well chosen initial configuration, a robot can better reach locations important to an assistive task despite model error, pose uncertainty and other sources of variation. However, finding effective configurations can be challenging due to complex geometry, a large number of degrees of freedom, task complexity and other factors. We present task-centric optimization of robot configurations (TOC), which is an algorithm that finds configurations from which the robot can better reach task-relevant locations and handle task variation. Notably, TOC can return more than one configuration that when used sequentially enable a simulated assistive robot to reach more task-relevant locations. TOC performs substantial offline computation to generate a function that can be applied rapidly online to select robot configurations based on current observations. TOC explicitly models the task, environment, and user, and implicitly handles error using representations of robot dexterity. We evaluated TOC in simulation with a PR2 assisting a user with 9 assistive tasks in both a wheelchair and a robotic bed. TOC had an overall average success rate of 90.6% compared to 50.4%, 43.5%, and 58.9% for three

We thank Henry and Jane Evans for providing input on assistive tasks and actuated beds. We also thank Daehyung Park and Zackory Erickson for their valuable feedback. This work was supported in part by the National Institute on Disability, Independent Living, and Rehabilitation Research (NIDILRR), grant 90RE5016-01-00 via RERC TechSAGE, and by NSF Awards IIS-1514258 and IIS-1150157. Dr. Kemp is a cofounder, a board member, an equity holder, and the CTO of Hello Robot, Inc., which is developing products related to this research. This research could affect his personal financial status. The terms of this arrangement have been reviewed and approved by Georgia Tech in accordance with its conflict of interest policies.

A. Kapusta
Georgia Institute of Technology E-mail: akapusta@gatech.edu

C.C. Kemp
Georgia Institute of Technology

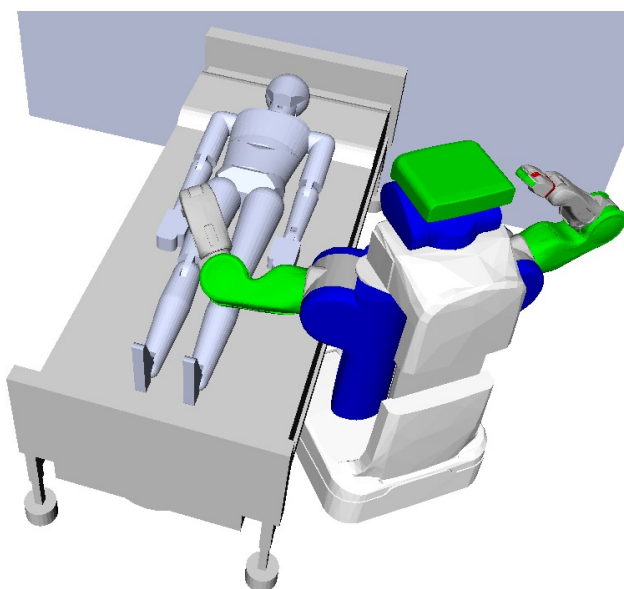


Fig. 1: TOC can select a configuration for the PR2 and the robotic bed so the PR2 can better reach task-relevant locations. This figure shows the configuration for the task of a PR2 cleaning the legs of a person in a robotic bed.

baseline methods from literature. We additionally demonstrate how TOC can find configurations for more than one robot and can be used to assist in designing or optimizing environments.

Keywords Mobile Manipulation · Assistive Robotics · Human-Robot Interaction · Robot Autonomy

1 Introduction

Robotic assistance with activities of daily living (ADLs) (Wiener et al, 1990) could potentially enable people to be more independent. This may improve quality of life (Vest et al, 2011; Andersen et al, 2004) and help address societal challenges, such as aging populations, high health care costs, and shortages of health care workers found in the United States and other countries (Institute of Medicine, 2008; Goodin, 2003).

Many specialized assistive devices can help people with motor impairments perform ADLs on their own (dev, 2015, 2017). Specialized robots, such as desktop feeding devices, have been successful for a narrow range of assistive tasks when placed in fixed and designated positions with respect to the user (Topping and Smith, 1998; Topping, 1999). The choice of where to place such robots is important, as it can impact the robot’s ability to provide effective assistance. General-purpose mobile manipulators have the advantage of mobility, which may allow them to provide assistance across a wide range of tasks, users, and environments (Chen et al, 2013). However, this mobility introduces additional complexity. For a mobile manipulator to provide assistance to a person, it may first need to get close and be able to reach task-relevant locations. For mobile manipulators, the problem of selecting the robot’s base pose may arise repeatedly as it moves around performing tasks. In this paper we use the more general term, configuration, which includes the robot’s base pose as well as other configurable parameters selected for the task (e.g., the height of the robot’s spine). Choosing the robot’s configuration can be challenging because of robot complexity, task complexity, geometric constraints, and kinematic constraints. Additionally, more than one configuration of the robot may be necessary to complete some tasks or more than one robot may be involved. For example, Hawkins et al (2014) used two positions of a PR2 (a mobile manipulator made by Willow Garage) to reach and shave the entirety of a user’s face (both sides) for a user in a wheelchair.

Our approach to providing assistance to a user with a robot is to first find a good configuration for the robot from which it can perform the task. In this work, we focus exclusively on the problem of selecting the robot configuration, leaving task performance out of scope. Performance of assistive tasks is addressed in many other works (see Section 2.4). The questions we ask are: how can the the robot select a good configuration, and what makes a configuration good? We address these questions in Section 3. With a good configuration, the robot is more likely to be able to complete the task successfully.

We present a task-centric, optimization-based method to select one or more configurations for assistive robots, that we call task-centric optimization of robot configurations (TOC). TOC extends two previous works from Kapusta et al (2015);

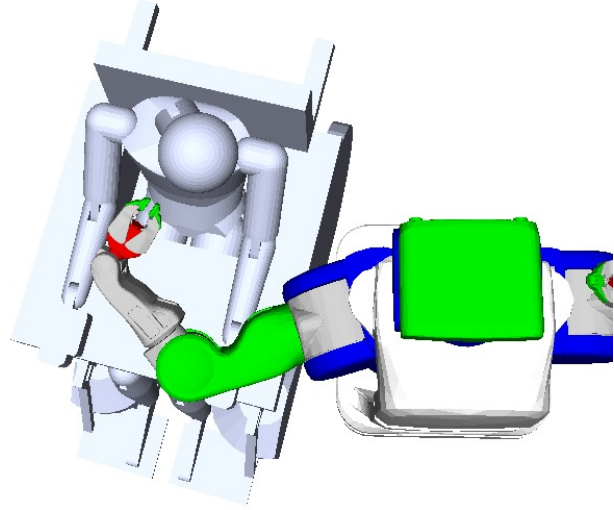


Fig. 2: TOC can select a single configuration for the PR2 to shave a person in a wheelchair, shown here. TOC takes advantage of the person’s physical capabilities, such as being able to rotate his or her neck.

Kapusta and Kemp (2016), with changes to framework, formulation of terms used within the methods, and modeling of the user and environment. Additionally, we have improved the optimization search and performed additional evaluations of our method with thorough comparisons to other methods from the literature. TOC is suitable for quickly selecting one or more robot configurations for assistive tasks, including some activities of daily living (ADLs), that involve the robot moving a tool around a person’s body. A task-centric approach is particularly applicable to assistive tasks where there may be important or common tasks that take place in environments that are known apriori. Key features of TOC are its selection of multiple configurations for a task, its task-centric approach, its explicit modeling of many task-specific parameters that are important to assistive tasks (possible because of the task-centric approach), its representations of robot dexterity, and its framework splitting offline and online computation.

TOC performs substantial offline computation to generate a function that can be applied rapidly online to select robot configurations based on current observations. These offline computations use explicit models of the task, environment, and user. Because offline modeling may be vulnerable to problems with error and mismatch between models and reality, TOC uses two representations of robot dexterity that we developed, task-centric reachability (TC-reachability) and task-centric manipulability (TC-manipulability), in its objective function to help it select robot configurations that are implicitly robust to error. TOC searches the robot config-

uration space to maximize its objective function, a linear combination of TC-reachability and TC-manipulability, using a simulation-based, derivative-free optimization from literature, covariance matrix adaptation evolution strategy (CMA-ES). Figures 1 and 2 show the configurations selected for the cleaning legs task for a user in bed and the shaving task for a user in a wheelchair, respectively.

We evaluated TOC in simulation with a PR2 assisting a user with 9 assistive tasks in both a wheelchair and a robotic bed. For our evaluations we implemented three baseline algorithms from literature. The first used an inverse-kinematics (IK) solver to select a configuration with a collision-free IK solution to all task-relevant goal poses. The second and third baselines used a capability map from Zacharias et al (2007) to select a configuration with high capability score to the goal poses. The third baseline also checked that a collision-free IK solution existed for each goal pose. We ran Monte-Carlo simulations of pose estimation error and found that TOC’s average success rate was higher than or comparable to baseline algorithms for each task. TOC had an overall average success rate of 90.6% compared to 50.4% for the IK solver, 43.5% for capability map, and 58.9% for capability map with collision checking. Additionally, we provide evidence that TOC’s objective function is positively correlate with robustness to error, and we demonstrate how TOC can be used to assist in designing environments to improve robotic assistance.

2 Related Work

2.1 Representations of Robot Dexterity

Many metrics have been developed to quantify the kinematic dexterity of robot manipulators. These metrics can be broadly divided into those that use the manipulator’s Jacobian, $\mathbf{J}(\mathbf{q})$ (Spong et al, 2006) and those that do not. These metrics can also be divided into those that find global measures (a metric for the robot irrespective of joint configuration) and those that find local, configuration-dependent measures of dexterity. Global dexterity metrics are often used for robot design (Stocco et al, 1998; Hammond and Shimada, 2011). As we are focused on dexterity measures to assist in positioning existing robots, we will focus on discussing local metrics. Yoshikawa (1984) proposed the local Jacobian-based metric called measure of manipulability (or just, manipulability), $w(\mathbf{q})$, shown in Equation 1.

$$w(\mathbf{q}) = \sqrt{\det(\mathbf{J}(\mathbf{q})\mathbf{J}(\mathbf{q})^T)} \quad (1)$$

Geometrically, manipulability is proportional to the volume of the manipulability ellipsoid of the manipulator, which is the volume of Cartesian space moved by the end effector for a unit ball of movement by the arm’s joints. This metric can be useful when assessing kinematic dexterity between

different configurations of the same robot. However, its scale and order dependencies make comparison between different robot morphologies challenging.

Other dexterity measures were developed that address some of the issues of using manipulability (Klein and Blaho, 1987). Kim and Khosla (1991) proposed another local Jacobian-based metric that we refer to in this paper as kinematic isotropy, $\Delta(\mathbf{q})$, shown in Equation 2.

$$\Delta(\mathbf{q}) = \frac{\sqrt[3]{\det(\mathbf{J}(\mathbf{q})\mathbf{J}(\mathbf{q})^T)}}{\left(\frac{\text{trace}(\mathbf{J}(\mathbf{q})\mathbf{J}(\mathbf{q})^T)}{3}\right)} \quad (2)$$

Kinematic isotropy uses the manipulability term (shown in Equation 1) with an alteration to remove order dependency and divided by a term to remove scale dependency. Order is the size of the Cartesian space of interest. For a planar robot, the order would be three if translations are all in 2D in-plane and in-plane rotations are considered. For the case of tasks in 6D space (position and orientation), the order is six. Unlike manipulability, the values of kinematic isotropy always range from 0 to 1 they can be directly compared across robot platforms. In our work we modified kinematic isotropy, adding a weighting term to create what we call joint-limit-weighted kinematic isotropy (JLWKI). We use JLWKI in our task-centric manipulability (TC-manipulability) defined in Section 3.7. TC-manipulability represents the kinematic dexterity of the robot for a task (a set of goal poses) from a set of one or more positions of the robot.

An important limitation to some Jacobian-based measures of dexterity is their ignorance of many relevant features of the workspace, such as joint limits and collisions. The manipulability ellipsoid calculated from the Jacobian suggests that the end effector can move in ways that may be constrained by joint limits. Many researchers have proposed various ways to include these features (joint limits: Tsai (1986); Chan and Dubey (1995); velocity limits: Lee (1997); torque limits: Hammond III and Shimada (2009)) into weighting terms. Vahrenkamp et al (2012) created what they called an extended manipulability measure by modifying the Jacobian to include weights on joint limits, on proximity to self-collision, and on proximity to collision with the environment. Many of these methods apply their weighting terms directly to manipulability or indirectly by modifying the Jacobian, which is used in manipulability. JLWKI differs from other measures of dexterity, using a distinct weighting function on joint limits and applying it to kinematic isotropy. JLWKI, does not include costs on proximity to collision because we found that calculating these costs increases the computation time of TOC excessively.

Zacharias et al (2007) introduced a method for representing manipulator dexterity without using Jacobians, which they use to score the workspace of a robot, creating what they

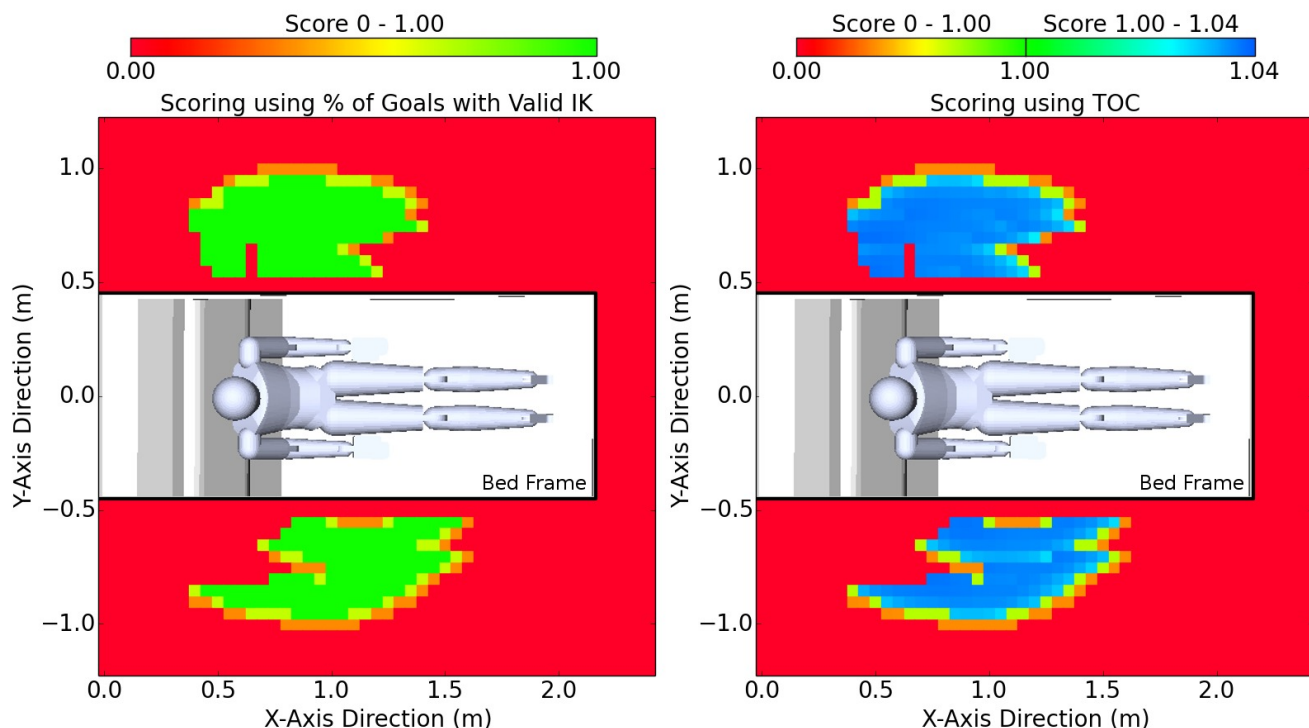


Fig. 3: TOC differentiates between robot configurations that have collision-free IK solutions to all goal poses. This differentiation allows TOC to better select good robot configurations. The figure visualizes two scoring methods, showing the score for discretized PR2 base poses. Z-rotation is sampled every 45° from 0° to 360° , and the best score is shown (left) using the percentage of goals with collision-free IK solutions and (right) TOC, for the mouth wiping task in the robotic bed environment, with the bed raised 20 cm and at 45° . The color represents the best score for that 2D position of the PR2. 0 means no goals and ≥ 1 means all goals have collision-free IK solutions.

call a capability map. To create the capability map they discretize space around the robot into 3D points and discretize the range of possible orientations around each 3D point. The capability score (also known as reachability score) is the number of orientations for which the robot has a valid IK solution. A way to interpret the meaning of this score is, if a goal pose is located at the 3D location, the capability score is similar to the probability that the manipulator can achieve the pose.

2.2 Selecting Robot Configurations for Mobile Manipulation

Prior research has investigated how to select configurations for a mobile robot. A common method is to address the problem using IK solvers (Diankov, 2010; Beeson and Ames, 2015; Kumar et al, 2010; Smits, 2006). The entire kinematic chain from end effector to the robot’s base location may be solved using IK (Gienger et al, 2005; Grey et al, 2016). Alternatively, sampling-based methods may be used to find robot base poses that have valid IK solutions, often as part of motion planning (Elbanhawi and Simic, 2014; Stilman and

Kuffner, 2005; Lindemann and LaValle, 2005; Garrett et al, 2015; Diankov et al, 2008).

By relying solely on IK to ensure that the robot can reach the goals, these methods are dependent on accurate models. Many of these methods are fast, but may fail if there is modeling or state estimation error. Like these methods, TOC uses a sampling-based search to find a robot configuration with valid IK solutions. However, there are many such robot configurations, and they cannot be distinguished using only IK, as shown in Figure 3(left). All locations in green have collision-free IK solutions to all goals, but some may result in higher success rates than others. TOC uses task-centric manipulability to differentiate those configurations, as shown in Figure 3(right). We show in Section 4.4 that higher TOC score is correlated with improved performance for configurations that have collision-free IK solutions to all goals. Additionally, TOC can find more than one robot configuration for a task. We implemented a standard IK sampling-based method as a baseline for comparison, as described in Section 4.2.

A body of work is based on the capability map from Zacharias et al (2007). Capability-map-based methods are

robot-centric and task-agnostic; they are generated offline for the robot’s manipulator and applied to tasks online. They typically select the robot base position by overlapping the capability map with end effector goal poses and maximizing the average capability score (Zacharias et al, 2009; Porges et al, 2014; Leidner et al, 2014).

Dong and Trinkle (2015) altered the capability map by creating an orientation-based capability map and extending the map for tools on the robot’s end effector. In contrast with our method, existing capability-map-based methods do not consider collisions with the environment in their offline computations because they do not model the environment. Collisions are only considered at runtime to eliminate robot base locations in collision or that lack collision-free IK solutions. Simply selecting the robot base location with highest capability map score is fast, but searching for a collision-free location can take more time. Capability-map-based methods also only find a single location for a robot for a task, but our method can find multiple robot configurations. We implemented two capability-map-based methods as baselines for comparison, based on Zacharias et al (2009), as described in Section 4.2.

Another body of work extends the capability map by inverting it, creating an inverse-reachability map. While a capability map scores end effector poses with respect to a robot base pose, the inverse-reachability map scores robot base poses with respect to an end effector pose. As with the capability map, the inverse-reachability map is generated offline for the robot’s manipulator and can be used quickly online. For an end effector 3D position, discretized robot base poses are scored based on the capability map score to that 3D position. The inverse-reachability map is used to rapidly sample a robot base position that can reach a set of goal end effector poses (Diankov and Kuffner, 2008; Burget and Bennewitz, 2015). Vahrenkamp et al (2013) used an alternative representation of the robot’s dexterity from their previous work (Vahrenkamp et al, 2012) that uses 6D poses in the workspace. They invert that workspace representation to create what they call an Oriented Reachability Map (ORM). ORM, like the inverse-reachability map, scores robot base poses based on the extended manipulability measure of each 6D pose in the manipulator’s discretized workspace. When searching for a robot base pose for a task, they sample in series from the ORM using the map’s score as a sampling weight. If the sampled robot base pose has collision-free IK solutions to the goal end effector poses, they use that base pose; if not they re-sample. They propose methods to incorporate task-specific information in their extended manipulability measure (and thus into the ORM), and to calculate the ORM map online through what they call lazy-ORM. Inverse-reachability-based methods and ORM differ from our work in a few ways. These methods are typically used in task-agnostic and robot-specific ways to facilitate applications of the robot to new tasks. No-

tably, these methods only find a single location for a robot for a given task, rather than multiple robot configurations. TOC also explicitly models features and parameters of the environment and user that may be important to assistive tasks. Details on this modeling is found in Sections 3.5 and 3.6.

Most previous task-centric methods use simulation of the task, with explicit error modeling, to evaluate robot base poses. Hsu et al (1999) presented a task-specific method for selecting a place for an industrial robot manipulator to perform a series of tasks amidst clutter. They used randomized path planners to generate collision-free paths for the arm and they randomly perturb the robot position to find positions from which the tasks can be performed quickly. Stulp et al (2009) present a task-centric method for finding areas in which to place a mobile manipulator where it can successfully perform a grasping task. They use Monte-Carlo simulation of error in the location of the object to be grasped to find base positions with high success rates. They simulate performance of the entire task including, navigation, motion planning and motion execution. For real-time base position selection, they convolve uncertainty in robot location with base position scores to provide an area of high-success probability. They used their method to select a 2D position of the robot base for a grasping task. These task-centric methods that explicitly model error and fully simulate task performance have only been used to select a few degrees of freedom in static environments, and can only select a single robot configuration for a task. In contrast, TOC uses faster, simpler simulation and implicitly handles error. TOC selects more degrees of freedom in configurable environments, and, again, can select multiple robot configurations for a task.

2.3 Human-robot Proxemics

Several bodies of work have examined the proxemics of human-robot interactions (Walters et al, 2011, 2009; Mumm and Mutlu, 2011; Takayama and Pantofaru, 2009; Walters et al, 2005).

Proxemics is the study of the spatial requirements of humans (e.g., the amount of space that people feel it necessary to set between themselves and others). These works look at acceptable interpersonal distances between humans and robots in social settings. Various works have used the concepts of human-robot proxemics to inform a robot when performing tasks. These works couple task performance concepts with scoring methods based on proxemics to select base positions and paths for the robot and item handover locations (Sisbot et al, 2010; Mainprice et al, 2011; Sisbot et al, 2006, 2007). Proxemics might suggest that placing the robot in front of the person at some minimum distance is preferred over other locations.

Kruse et al (2013) present a thorough survey of human-aware robot navigation. In contrast, TOC does not consider

proxemics or social factors; it instead focuses on kinematic aspects of the task. However, inclusion of additional terms in TOC’s objective function to include user comfort and proxemics is possible. While proxemics is often used to consider navigation problems, TOC focuses exclusively on selecting the configuration for the task, which may be the goal pose for navigation.

2.4 Assistive Robots

Researchers have investigated the use of mobile manipulators as assistive devices (Dario et al, 1999; Schaeffer and May, 1999; Graf et al, 2009; Bien et al, 2004; Jain and Kemp, 2010; Hawkins et al, 2014).

We seek to further empower assistive mobile manipulators by autonomously selecting configurations from which they can better provide assistance. This autonomy can improve task performance and decrease cognitive workload for teleoperated assistive systems, as from Grice and Kemp (2016). In this work, we have used a model of a robotic bed that matches Autobed, a robotic modified hospital bed from Grice et al (2016). We have shown how TOC can optimize the configuration of the bed, allowing improved assistance from a mobile manipulator as part of a collaborative assistive system, as from Kapusta et al (2016). This capability is demonstrated in our evaluations in the robotic bed environment in Section 4.2.

3 Task-centric Optimization of Robot Configurations (TOC)

As mentioned in Section 1, key features of task-centric optimization of robot configurations (TOC) are its task-centric approach, representations of robot dexterity, selection of multiple configurations for a task, and framework that splits offline and online computation. TOC is suitable for situations when tasks and environment layouts are known beforehand and we would like to configure the robot for these tasks such that the robot is successful despite variations between models and reality. By taking a task-centric approach, TOC is able to use task-specific knowledge, such as explicit modeling of task-relevant parameters, to better select configurations. We will first explain the goal of TOC. Afterwards we describe the nomenclature used in the remainder the paper. We then explain the framework of TOC, details of its features, and specifics of our implementation.

3.1 TOC Goal: Selecting Good Configurations

The goal of TOC is to select a good set of one or more configurations for a robot to perform a task without additional

adjustments. But what constitutes a *good* robot configuration? In this paper we use the term *robot configuration* as a more general term for the pose of the robot’s base, so it can include additional relevant parameters. For example, for a PR2, the robot configuration might be the position and orientation of the robot’s mobile base as well as the z-axis spine height of the robot. If the PR2 were operating in a room with a robotic bed, the degrees of freedom (e.g., the height of the bed) of the bed could be included in the robot configuration. We consider robot configurations in sets that can be of cardinality 1 or greater; the robot can complete the entire task by adopting all configurations in the set in any order. With a *good* set of configurations, the robot is more likely to be able to complete the task successfully. We judge the robot’s ability to perform the task from a set of robot configurations with one measure: if it can reach all goal poses collision-free with its end effector. Various forms of error, such as modeling error or state estimation error, may cause the robot to be unable to perform the task. Because the robot does not know how the modeling and state estimation error will manifest a priori, from a good set of robot configurations, the robot should be able to perform the task despite such error.

3.2 Nomenclature

c :	A task identifier
N_c :	The number of goal poses for task c
\mathbf{q} :	A joint configuration of the robot arm. $\mathbf{q} \in \mathbb{R}^n$, where n is the number of DoF of the arm
q_i :	The value for joint i in joint configuration \mathbf{q} , $\mathbf{q} \in \mathbf{q}$
$\mathbf{q}^-, \mathbf{q}^+$:	A list of the minimum and maximum values, respectively, for the joints of a robot’s arm.
q_i^-, q_i^+ :	The minimum and maximum values, respectively, for joint i of a robot’s arm.
\mathbf{r} :	A set of robot configurations of cardinality ≥ 1 , $\mathbf{r} = \{r_1, r_2, \dots, r_n\}$, where n is the number of robot configurations in set \mathbf{r}
$\hat{\mathbf{r}}^*$:	The estimated optimal robot configurations given current observations, the output of the online portion of TOC.
\mathbf{h} :	The set of uncontrollable parameters, discretized into $\{h_1, h_2, h_3, \dots\}$
$\hat{\mathbf{h}}$:	The uncontrollable parameters observed and estimated at run-time, the input to the online portion of TOC.
\mathbf{b} :	The set of free parameters, discretized into $\{b_1, b_2, b_3, \dots\}$

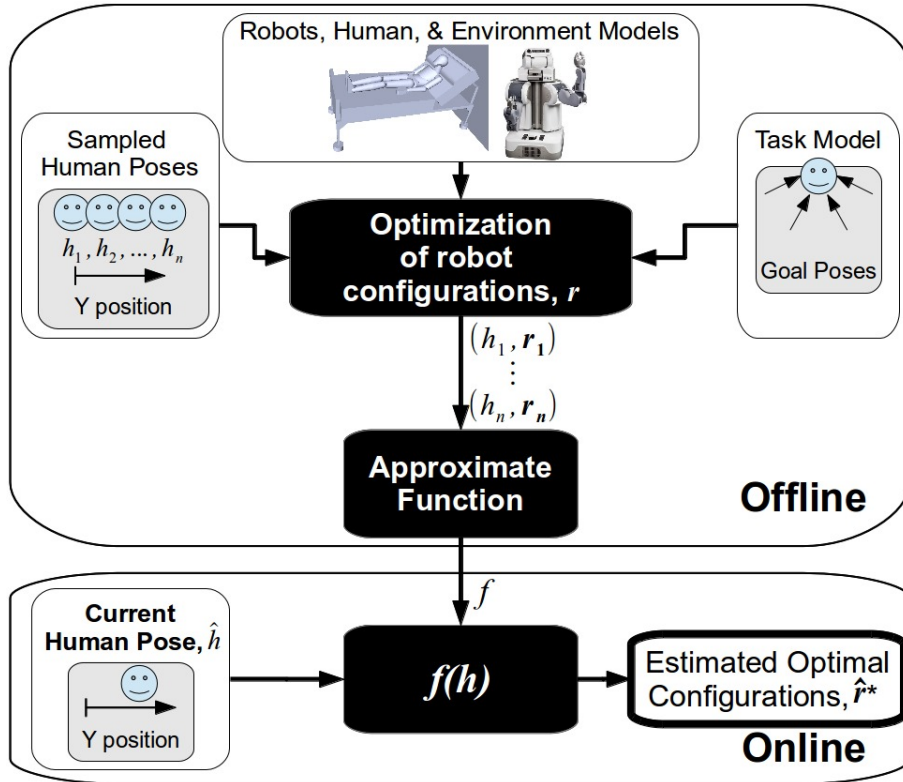


Fig. 4: The Framework used in TOC. The offline portion of TOC takes as input task-relevant models and samples of the uncontrollable parameters and outputs optimized robot configurations. It then approximates a function that is used online to estimate the optimal robot configurations given the current, observed uncontrollable parameters.

- \mathbf{x} : Set of position and orientation end effector goal poses $\mathbf{x} \in \mathbb{R}^6$. \mathbf{x} depends on c , h , and b , but we omit those for simplicity in writing. $\mathbf{x} = \{x_1, x_2, \dots, x_{N_c}\}$.
- $\mathbf{s}_{r,x}$: Set of IK joint configuration solutions to goal \mathbf{x} from robot configuration r , $\mathbf{s}_{r,x} = \{q_1, q_2, \dots, q_n\}$, where n is the number of IK solutions
- a : The order of the robot arm. In our case, 6.
- $\mathbf{J}(\mathbf{q})$: The Jacobian of the arm in joint configuration \mathbf{q}
- $\Delta(\mathbf{q})$: The kinematic isotropy for the arm in joint configuration \mathbf{q}
- f : A function that takes \hat{h} as input and outputs \hat{r}^* . TOC generates f offline and applies it online.

3.3 Framework

Figure 4 shows the framework of TOC for our implementation described in Section 4 for a person on a robotic bed. TOC performs most of its computation offline to approximate a function that can be used online to select robot configurations for a task. The optimization takes as input task-relevant

models (e.g., task, robot, user, and environment models) and a sample of the uncontrollable parameters (e.g., the position of the person on the bed), h . It outputs an optimized robot configuration, r , for that h . The inputs and outputs of the optimization are used to approximate the function, f that takes as input at run-time the observed estimated uncontrollable parameters, \hat{h} and outputs the estimated optimal configurations, \hat{r}^* .

3.4 Task Modeling

Our aim with task modeling is to create a representation that allows TOC to efficiently evaluate a robot's ability to perform a task. There are many tasks that consist of manipulation of small objects or tools around a person's body, that we expect can be well modeled by a set of goal poses (Cartesian positions and quaternion orientations) with respect to relevant reference frames. We manually model each task as a sparse set of poses for the robot's end effector. For example, Figure 5 shows the eight goal poses with respect to the person's head that make up our model of a shaving task. We assume that if the robot can reach all goal poses, it is likely to be able to perform the task. However, we expect there to be differences between the models and the real tasks. We consider

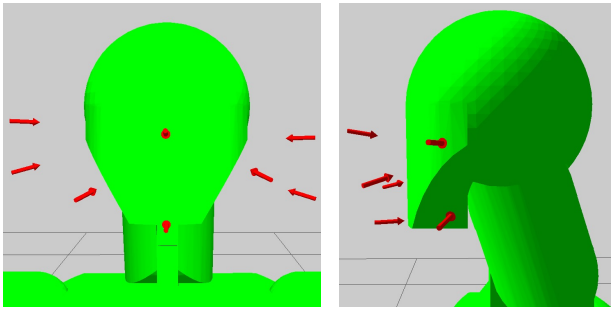


Fig. 5: The manually selected goal poses for the shaving task. Each arrow represents a position and orientation, 6-DoF end effector goal pose, with respect to the head. This shows views from the front and side.

these discrepancies to be a form of modeling error that TOC accounts for when selecting robot configurations.

3.5 Environment Modeling

Using its environment model, TOC finds robot configurations that avoid collision and unwanted interaction with obstacles, such as a bedside table or walls. TOC can use different resolutions for its environment model depending on the needs of the task. A room could be represented simply as a wall behind the bed, as shown in Figure 1, or it could contain models of furniture and other potential obstacles. The resolution of each object model could range from a block to a detailed mesh. TOC uses three types of objects to model the environment:

- Fixed objects
- Controllable movable/configurable objects
- Uncontrollable movable/configurable objects

TOC treats fixed objects as static obstacles in the world, to be avoided by the robot. We add the configuration of the controllable objects to the robot configuration space that TOC optimizes. An example of a controllable object is an adjustable bed. For uncontrollable objects, TOC selects a robot configuration for a sample of the possible configurations of the objects. For each sample of its configuration, the object is considered static. An example of an uncontrollable object is a nightstand that is not movable by the robot, but could be moved somewhere by a person prior to the robot starting the task. Using controllable and uncontrollable movable objects, TOC can suggest alterations to the environment that may improve task performance. Uncontrollable movable objects can also be used to generate robot configurations for possible states of the environment. This may be beneficial for environments, such as hospitals, where there are a few possible room layouts, but the robot may not know which layout will be relevant until it reaches the room.

Because TOC does not include a cost in proximity to collision between the robot and the environment in its objective function, we include a margin of safety in the environment model by expanding the environment model (we used ~ 3 cm in our evaluations). This safety margin reduces the risk of collision in the case of model or state estimation error, without having to explicitly include closeness to collision in the objective function.

3.6 User Modeling

TOC’s user model can be customized for a user to better locate relevant parts of the body, and to allow more accurate collision-checking. In our evaluation of TOC we used a mesh model of a human designed around a 50 percentile male from Tilley (2002), shown in Figure 1. TOC uses three types of parameters for the person’s configuration:

- Environment-driven parameters
- Uncontrollable parameters
- Free parameters

Environment-driven parameters are set according to the state of the environment. For a chair, the user’s body would be in a seated configuration. For a flat bed, the user’s body would be in a supine configuration. For a bed with an adjustable back rest, the user’s configuration would depend on the angle of the back rest. Uncontrollable parameters are treated similar to uncontrollable movable objects. TOC selects a robot configuration for a sample of the uncontrollable parameter. An example of an uncontrollable parameter is the position of the user on the bed, if the robot is unable to shift the body on the bed. Free parameters are used by TOC freely without including it in the robot configuration. An example of a free parameter used is the user’s neck rotation. Figure 2 shows a configuration of the PR2 that takes advantage of the user’s neck rotation to reach all goals for the shaving task in a wheelchair.

Just as with the environment model, we include a margin of safety in the human model by expanding the model.

3.6.1 Additional User Customization

TOC can consider additional customizations for the user’s needs or preferences. For example, a user may prefer certain angles of the bed’s head rest for feeding tasks. This preference can be represented as limitations or costs on the robot’s configuration space.

3.7 Configuration Scoring

Implicitly handling variation and error is a key aspect of TOC, because its heavy computation is performed offline for

models that may differ from reality. TOC uses two metrics that we have developed to estimate how well the robot will be able to perform the task from a set of configurations: task-centric reachability (TC-reachability) and task-centric manipulability (TC-manipulability).

3.7.1 Task-centric Reachability

Task-centric Reachability (TC-reachability), P_R , is the percentage of goal poses to which the robot can find a collision-free IK solution from robot configurations, \mathbf{r} , for a task c and uncontrollable parameters h , as shown in Equation (3).

$$P_R(\mathbf{r}, c, h) = \left(\frac{1}{N_c}\right) \sum_{k=1}^{N_c} \max_{r \in \mathbf{r}, b \in \mathbf{b}} W(r, x_k), \quad (3)$$

where

$$W(r, x_k) = 1 \quad \forall s_{r, x_k} \neq \emptyset,$$

and (4)

$$W(r, x_k) = 0 \quad \forall s_{r, x_k} = \emptyset.$$

Recall that \mathbf{x} depends on c , h , and b , but we omit those for simplicity in writing and N_c is the number of goal poses for task c . Note that $s_{r, x_k} \neq \emptyset$ means that the IK solver can find a collision-free solution to the goal pose x_k from robot configuration, r .

TC-Reachability is related to using an IK solver with collision checking, but with the additional functionality of evaluating sets of robot configurations.

3.7.2 Task-centric Manipulability

Task-centric Manipulability (TC-manipulability), P_M , is related to the average kinematic dexterity of the arm when reaching the goal poses. It is defined here differently from our previous works, such as from Kapusta et al (2015).

TC-manipulability score is based on kinematic isotropy (Kim and Khosla, 1991), shown in Equation (2). Kinematic isotropy only considers the Jacobian of the arm in a configuration, ignoring potentially relevant properties of the robot arm, such as joint limits. When at a joint limit, the arm cannot move in one direction, effectively halving the movement of that joint. Hammond III and Shimada (2009) used torque-weighted global isotropy index and torque-weighted kinematic isotropy to estimate the dexterity of a robotic arm given joint torques and torque limits. Vahrenkamp et al (2012) investigated configuration-based weighting functions to create what they call an augmented Jacobian that they use in manipulability. We have similarly modified kinematic isotropy to consider joint limits by scaling the manipulator's Jacobian by an $n \times n$ diagonal joint-limit-weighting matrix \mathbf{T} , defined

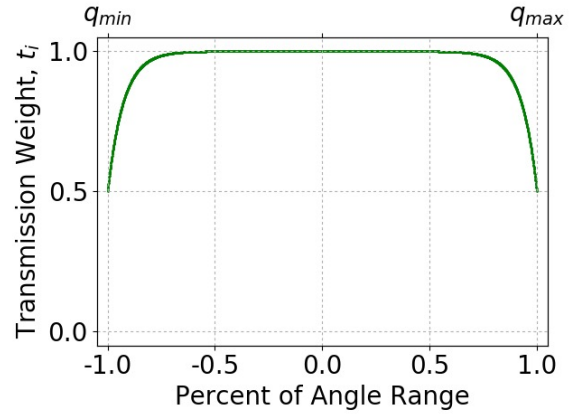


Fig. 6: A plot of the joint-limit weighting function ranging from maximum joint value to the minimum joint value.

in Equation 5, where n is the number of joints of the manipulator.

$$\mathbf{T}(\mathbf{q}, \mathbf{q}^-, \mathbf{q}^+) = \begin{bmatrix} t_1 & 0 & 0 \\ 0 & \ddots & 0 \\ 0 & 0 & t_n \end{bmatrix} \quad (5)$$

t_i in \mathbf{T} is defined as

$$t_i = 1 - \eta^\kappa$$

where

$$\kappa = \frac{q_i^r - |q_i^r - q_i + q_i^-|}{\zeta q_i^r} + 1 \quad (6)$$

and

$$q_i^r = \frac{1}{2}(q_i^+ - q_i^-).$$

We set $t_i = 1$ for infinite roll joints. The variable η is a scalar value that determines the maximum penalty incurred when joint q_i approaches q_i^+ or q_i^- and ζ determines the shape of the penalty function. We used a value of 0.5 for η and $\frac{1}{20}$ for ζ . This weighting function and the values for η and ζ were selected to halve the value of the kinematic isotropy at joint limits, have little effect in the center of the joint range, to begin exponentially penalizing joint values beyond 75% of the range, and to operate as a function of the percentage of the joint range. Fig. 6 shows the value of t_i as a function of the joint value as a percentage of its joint range.

We then define joint-limited-weighted kinematic isotropy (JLWKI) as

$$\text{JLWKI}(\mathbf{q}) = \frac{\sqrt{\det(\mathbf{J}(\mathbf{q})\mathbf{T}(\mathbf{q}, \mathbf{q}^-, \mathbf{q}^+)\mathbf{J}(\mathbf{q})^T)}}{\left(\frac{1}{n}\right)\text{trace}(\mathbf{J}(\mathbf{q})\mathbf{T}(\mathbf{q}, \mathbf{q}^-, \mathbf{q}^+)\mathbf{J}(\mathbf{q})^T)}. \quad (7)$$

We use a function, F , to find the maximum value of $\text{JLWKI}(\mathbf{q})$ for robot configuration r and goal pose x_k , where

$$F(r, x_k) = \max_{q \in \mathcal{S}_{r, x_k}} \text{JLWKI}(q) \quad \forall \mathcal{S}_{r, x_k} \neq \emptyset, \quad (8)$$

and

$$F(r, x_k) = 0 \quad \forall \mathcal{S}_{r, x_k} = \emptyset.$$

We finally define TC-manipulability, P_M , as

$$P_M(\mathbf{r}, c, h) = \left(\frac{1}{N_c}\right) \sum_{k=1}^{N_c} \max_{r \in \mathbf{r}, b \in \mathbf{b}} F(r, x_k). \quad (9)$$

3.8 Optimization

TOC’s optimization takes as input task-relevant models for task, c , and a sample of the uncontrollable parameters, h . It outputs an optimized set of robot configurations, \mathbf{r} . TOC runs this optimization for samples of the uncontrollable parameters for each task. TOC searches the robot configuration space to maximize its objective function, a linear combination of TC-Reachability and TC-Manipulability, shown in Equation 10.

$$\arg \max_{\mathbf{r}_i} \alpha P_R(\mathbf{r}_i, h_i, c) + \beta P_M(\mathbf{r}_i, h_i, c) \quad (10)$$

Both TC-reachability and TC-manipulability range from 0 to 1, allowing them to be directly compared in the optimization. We selected a value of 1 for α . We chose to define β as

$$\beta(\mathbf{r}) = (0.1)(0.95)^{n-1} \quad (11)$$

where n is the cardinality of \mathbf{r} . In our implementation of TOC the cardinality of \mathbf{r} was 1 or 2. These definitions of α and β emphasize the importance of reaching goals over being able to reach around goals, and includes a small penalty in the objective function’s value for using more configurations. There are often many configurations that can reach all goals. TC-manipulability is used to differentiate between these configurations. As an example, we compare TOC to a standard method from literature: using an IK solver with a collision checker to find a robot configuration that can reach all goals. Figure 3 shows the difference in scoring between using the existence of IK solutions for scoring and using TOC for scoring for a task for a user in bed. Figure 3 (left) shows that many poses of the robot’s base have the same score, each having collision-free IK solutions to all goals. Figure 3 (right) shows scoring using TOC, where TC-manipulability allows additional differentiation between robot base poses that can reach all goals. Higher TC-manipulability is correlated with mean accuracy (percentage of goals that are reachable), as we show in Section 4.4.

3.8.1 Search Method

The space of the objective function can be highly nonlinear and challenging to search. There are several derivative-free, simulation-based optimization methods that could be applied to this problem. A simple method would be to uniformly sample the space and select the configuration with highest objective function value. However, we found that uniform sampling had difficulty finding good configurations for tasks where the solution space was small. Tan et al (2011) used Covariance Matrix Adaptation Evolution Strategy (CMA-ES) to design a controller for articulated bodies moving in a hydrodynamic environment, which inspired our use of CMA-ES (from <https://pypi.python.org/pypi/cma>) for our optimization. We used a heuristic when both P_R and P_M are zero that pushes the search toward configurations that may have non-zero P_R and P_M . All values of the heuristic are less than 0.

3.9 Approximate Function

Offline, TOC approximates a function that takes as input an estimation of the uncontrollable parameters, \hat{h} , such as the location of the person on the bed, and outputs the estimated optimal robot configurations, $\hat{\mathbf{r}}^*$. At run-time, TOC applies this function to the observed, estimated uncontrollable parameters. For this paper we used K-nearest neighbor (K-NN) with $K = 1$ (hence, 1-NN) as the function, f . We trained the 1-NN algorithm with a set of (h, r) pairs and it returns as $\hat{\mathbf{r}}^*$ the r for the h that is closest to \hat{h} . In our implementations of TOC we trained the 1-NN on fewer than 20 (h, r) pairs for each task and found that the 1-NN would return $\hat{\mathbf{r}}^*$ in less than 1 second.

4 Evaluation

4.1 Implementation

We manually created models for 9 assistive tasks: shaving, feeding, wiping the mouth, cleaning both arms, cleaning both legs, and scratching the left/right upper arm, and left/right knee (each scratching task was considered separately). Previous work has noted that these types of tasks may be useful for those with severe motor impairments (Chen et al, 2013). As described in Section 3.4, task models consisted of a set of goal poses, each of which was a position and orientation goal for the robot’s end effector. We defined each goal pose with respect to a relevant reference frame (e.g., the head for shaving, or the shoulder for scratching the upper arm), so they move appropriately as the model parameters change (e.g., the height of the bed). We chose these tasks as representative of

various activities for which a robot like the PR2 may be able to provide assistance to a user with motor impairments.

For example, Figure 5 shows the eight goal poses with respect to the person’s head that we selected to model the shaving task. For simplicity, we limited tasks to one-handed tasks and used only the robot’s left arm in our evaluations. In our implementation we allowed TOC to search for sets of robot configurations of cardinality 1 or 2. When exploring multiple robot configurations for a task, we assume the robot can move from one configuration to another.

We ran all simulations in OpenRAVE (<http://www.openrave.org/> from Diankov and Kuffner (2008)), for which we created environment models with a PR2 robot and a model of an average male human placed either in a wheelchair or in a robotic bed. The human model dimensions come from Tilley (2002). The PR2 is a mobile manipulator made by Willow Garage with two 7-DoF arms. The models we created for the robotic bed and the wheelchair match Autobed, a modified Invacare 5401IVC full electric hospital bed (Grice et al, 2016) and a Sunrise Medical Quickie 2 wheelchair with overlap table, respectively. The casters on the bed and wheelchair are represented by swept volumes. For the wheelchair, we removed the part of the casters’ swept volumes that extends to the sides of the chair to increase free space around the chair. We assume that the user would ensure that the casters are not pointing out from the chair.

Figure 7 shows the configurations selected by our implementation of TOC for each task, given the observation, \hat{h} , that the person was positioned in the center of the bed or wheelchair.

The robotic bed environment has the bed in front of a wall, to emulate how beds are often positioned in rooms. The robotic bed can raise up to 25 cm and can increase the angle of its head rest up to 75°. For the wheelchair environment we gave the human the ability to rotate its neck up to 45° in either direction about the Z-axis. Figure 2 shows the neck rotated 45°. These two environments (robotic bed and wheelchair) were selected to demonstrate many of the functionalities of the TOC framework. The robotic bed environment demonstrates how TOC can select configurations for multiple robots in the environment, how TOC can handle controllable and uncontrollable parameters of the environment, and how it handles uncontrollable and environment-driven parameters of the user. TOC treats additional robots the same as controllable objects, adding their parameters to the robot configuration, as it does with the robotic bed’s parameters. TOC considers the position of the person on the bed as an uncontrollable parameter and considers the other parameters of the user (the configuration of the person’s joints) as environment-driven parameters. The wheelchair environment demonstrates how TOC can make use of free parameters in the user model. TOC considers the rotation of the person’s neck as a free parameter.

4.2 Evaluation Against Baselines

We compared the performance of TOC against three baseline methods in Monte Carlo simulations of Gaussian error introduced in the person’s position (e.g., translating around on the bed while the bed remains stationary) and in the robot’s base pose (e.g., translating and rotating the robot from the selected robot configuration). Each method estimated an optimal set of robot configurations, \hat{r}^* , given the observation, \hat{h} , that the person was positioned in the center of the bed or wheelchair. Because the goals are sparse and represent a more complicated task, we considered a trial successful if, from the robot configurations selected by the method, the PR2 could reach all goal poses despite the error introduced in the Monte Carlo simulation. Otherwise, the trial was a failure. We performed this evaluation for all 9 modeled tasks in both environments except the cleaning legs tasks for the wheelchair environment because the overlap table blocks access to the thighs, preventing successful performance of the task.

All introduced error was normally distributed around 0. For the robotic bed environment, the standard deviation for the human’s pose was 2.5 cm translation in the global X direction and 5.0 cm translation in the global Y direction. Rotations of the human in bed were not considered because small rotations about the head results in large movements of the legs. For the wheelchair environment, the standard deviation for the human’s pose was 2.5 cm translation in the global X direction, 5.0 cm translation in the global Y direction, and 5° rotation about the human head’s Z axis. The standard deviation for the PR2’s position was 1.0 cm in the global X and Y directions and 5° rotation about the robot’s Z axis. We selected these error distributions from typical error in human pose estimation and PR2 servoing in our previous work (Kapusta et al, 2016). As described in Sections 3.5 and 3.6, models used for selecting configurations had a small safety margin of ~ 3 cm. Models used for testing had no safety margin.

For fair comparison, all methods in this evaluation were given matching seeds for their optimization via CMA-ES as well as for their error in Monte-Carlo simulation. For the CMA-ES optimization, all methods were given a population size of 40, a maximum number of iterations of 1000, and the opportunity to restart with double the population if the optimization ran out of iterations before converging within some tolerance. All methods also had the same heuristics for driving the search towards configurations that may have collision-free IK solutions. We assigned appropriate bounds on parameters based on the environment (e.g., slightly beyond reach of the bed). We initialized the parameters to aid coverage in the search, giving two initial locations, one position on one side of the bed or wheelchair and one on the other side. Baseline methods were allowed two searches, one for each initialization, and selected the single best configura-

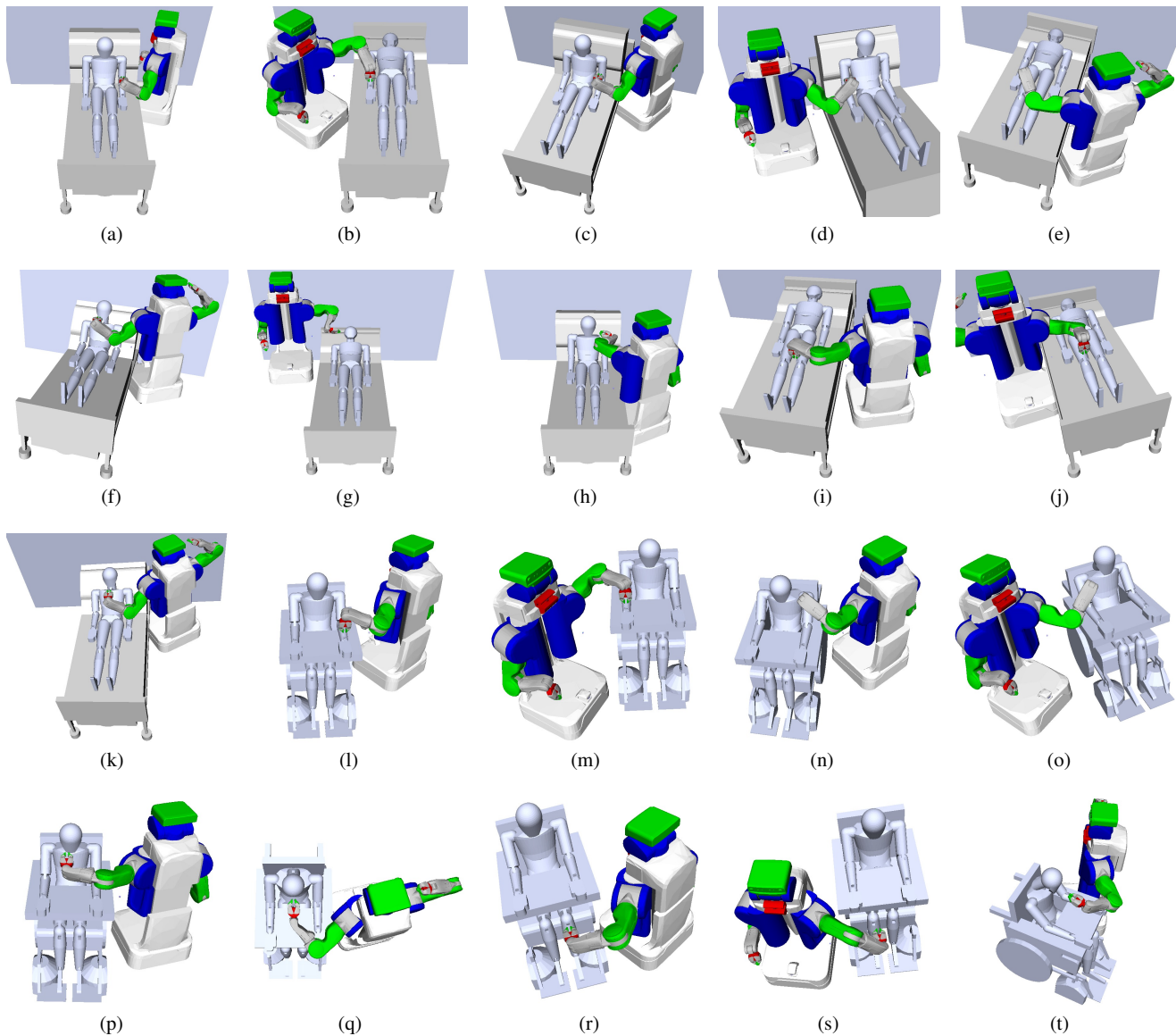


Fig. 7: Visualization of the robot configurations selected by TOC for each task. Two images are used when TOC selected two configurations for a task task. The images show for the robotic bed environment: (a) cleaning arms config #1 (b) cleaning arms config #2 (c) scratching left upper arm (d) scratching right upper arm (e) cleaning legs (f) wiping mouth (g) shaving config #1 (h) shaving config #2 (i) scratching left knee (j) scratching right knee (k) feeding. The images show for the wheelchair environment: (l) arm cleaning config #1 (m) arm bed config #2 (n) scratching left upper arm (o) scratching right upper arm (p) wiping mouth (q) shaving (r) scratching left knee (s) scratching right knee (t) feeding.

tion. TOC jointly optimized its two configurations from their respective initialization locations. Thus, all methods were given the comparable initializations and bounds.

4.2.1 Baselines

We implemented three baselines from literature to compare against TOC, one based on IK and two based on the robot capability map. An overview of these and other related methods

from literature can be found in Section 2. These methods selected a single configuration for both the PR2 and the robotic bed and made use of the human's free parameter (neck rotation) in the wheelchair environment.

Inverse-Kinematics (IK) Solver-based Baseline IK solver-based methods to select a robot base pose for a task are common in literature. The method we implemented uses CMA-ES to search for a robot configuration where the robot

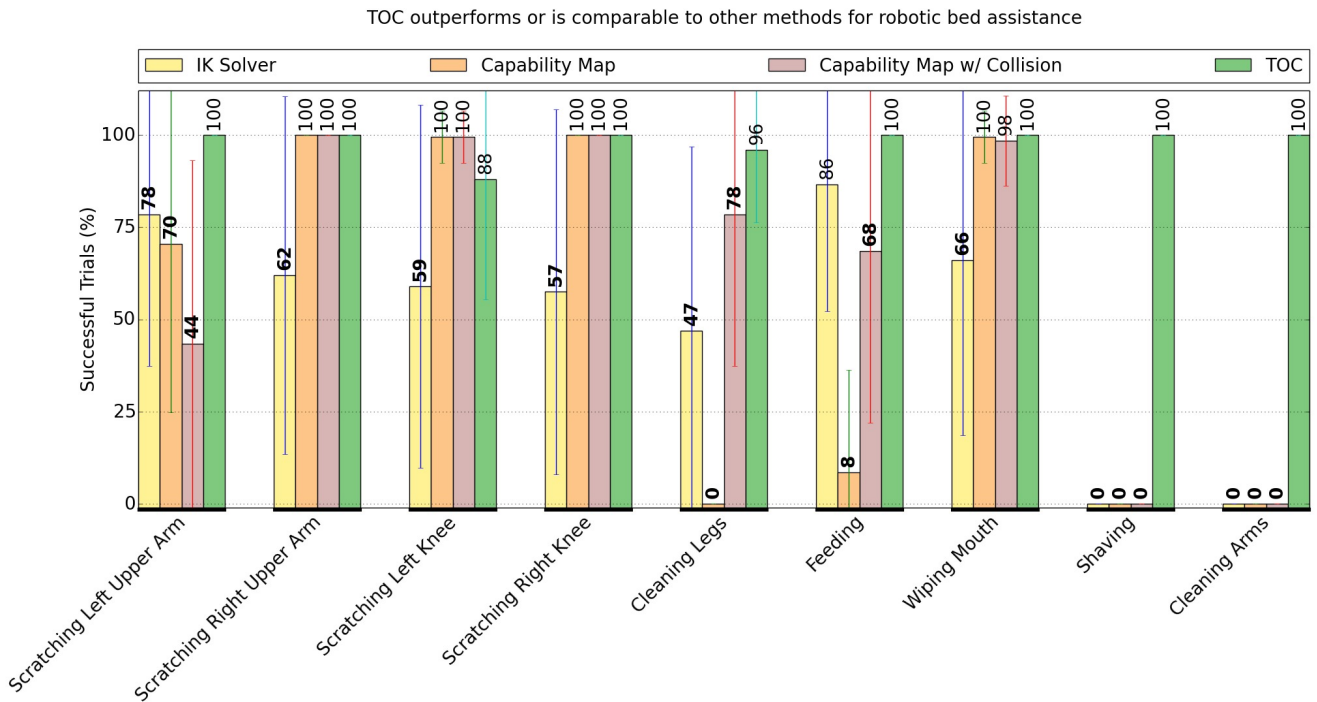


Fig. 8: Comparison of performance between TOC and three baseline methods averaged over 200 Monte-Carlo simulations of state estimation error for tasks in the robotic bed environment. Bold numbers have statistically significant ($p < 0.01$) difference from the TOC result in a Wilcoxon Rank-Sum test. Error bars show one standard deviation. TOC chose to use a single configuration for all tasks other than the shaving and cleaning arms tasks in this environment. Baseline methods could only select a single configuration.

has a collision-free IK solution to all goal end effector poses. We used the `ikfast` module within the OpenRAVE simulation environment to determine if a collision-free IK solution existed for each robot configuration.

Capability Map-based Baselines Various methods from literature use the capability map Zacharias et al (2007). We implemented two baseline methods roughly based on Zacharias et al (2009). For these methods we first created a capability map using OpenRAVE’s kinematic reachability module. To create the capability map, the module discretized 3D space around the robot’s arm into 3D points and discretized the range of possible orientations around each 3D point. The capability score (also known as reachability score) for each point is the percentage of orientations for which the robot has a valid IK solution. These scores are calculated offline and saved. These two methods use CMA-ES to search for a robot configuration that maximizes the average capability score for all goal poses. The score of a goal pose is the score of the closest 3D point from the capability map. The first capability map-based baseline considered capability scores without regard to the environment. The second gave goal poses a 0 score if a collision-free IK solution could not be found to that pose in the environment.

4.2.2 Results

The results for each task for the robotic bed and wheelchair are shown in Figures 8 and 9, respectively. TOC’s average success rate was higher than or comparable to baseline methods in all tasks. Statistically significant difference from the TOC result ($p < 0.01$ in a Wilcoxon Rank-Sum test) is indicated in the figures with bold numbers.

TOC had an overall average success rate of 90.6%, compared to 50.4% for IK, 43.5% for capability map, and 58.9% for capability map with collision checking. The overall differences between baseline results and TOC are statistically significant ($p < 0.01$) in a Wilcoxon Rank-Sum test. TOC chose to use a single configuration for all tasks other than the shaving and cleaning arms tasks in this environment in the bed environment and it used a single configuration for all but the cleaning arms task in the wheelchair environment. TOC achieved higher average success rates both for tasks for which it used one and two configurations. This result suggests that benefit from TOC comes from more than just from using 2 configurations over one. For tasks that require more than one robot configuration, baseline methods failed; they could only select a single configuration. TOC jointly

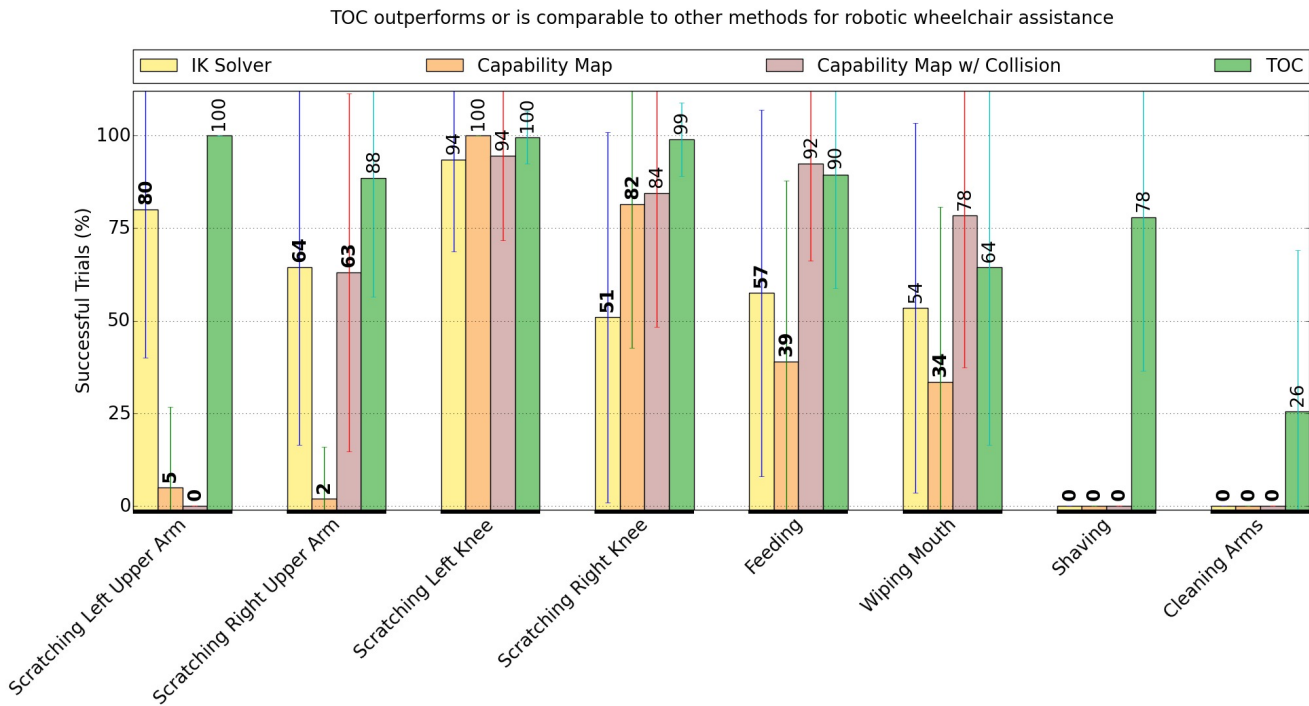


Fig. 9: Comparison of performance between TOC and three baseline methods averaged over 200 Monte-Carlo simulations of state estimation error for tasks in the wheelchair environment. Bold numbers have statistically significant ($p < 0.01$) difference from the TOC result in a Wilcoxon Rank-Sum test. Error bars show one standard deviation. TOC chose to use a single configuration for all tasks other than the cleaning arms task in this environment. Baseline methods could only select a single configuration.

optimizes 2 configurations, allowing it to succeed in these challenging tasks.

4.3 Quantifying Robustness

In Figures 10, 11 and 12 We visualize the robustness of robot configurations selected by TOC for the shaving and cleaning arms tasks in the two environments. These figures show the percentage of goal poses that have collision-free IK solutions (indicated by the color) for varying error in the person’s position on the bed or wheelchair (the X-Y axes). Notable in these figures is the success region in blue, where all goals are reachable, as well as how the two configurations combine to reach all goals. For pose estimation error in the success region, the PR2 would still be able to successfully perform the task. TOC opted to use two configurations for each of the tasks shown. The success region is large and surrounds the origin for shaving and cleaning arms in bed, which is why 100% of the trials were successful for these tasks in Figure 8. The success region is less centered around the origin for the cleaning arms task in the wheelchair, hence its lower percentage of successful trials in Figure 9. The Monte Carlo simulations randomly sampled in these, as well as other, degrees of freedom and sampling outside the success

region results in a failed trial. These figures suggests that the task may be easier for the robot to perform for a person in bed. Closer observation of the task shows that, because the wheelchair is tall, the goals poses for the cleaning arms task are vertically higher in the PR2’s workspace and the arm have relatively low JLWKI when reaching those goals.

4.4 Evaluation of TOC Objective Function

TOC searches for a set of robot configurations that maximizes its objective function, which we will call its score for simplicity. The assumption therein is that higher values of the score are correlated with better robot configurations, that are more robust to error. To test this assumption, we evaluated the relationship between the TOC score and the accuracy (the percentage of goals that are reachable) for robot configurations in the same evaluation described in Section 4.2. Note that we chose to compare against accuracy in this evaluation because it can convey more information than success, which is binary. A similar correlation can be seen for success. For the wiping mouth task in the robotic bed, we sampled robot configurations with TC-reachability of 1 (i.e., all goal poses have collision-free IK solutions) and compared their mean and variance in accuracy over 200 Monte Carlo simulations

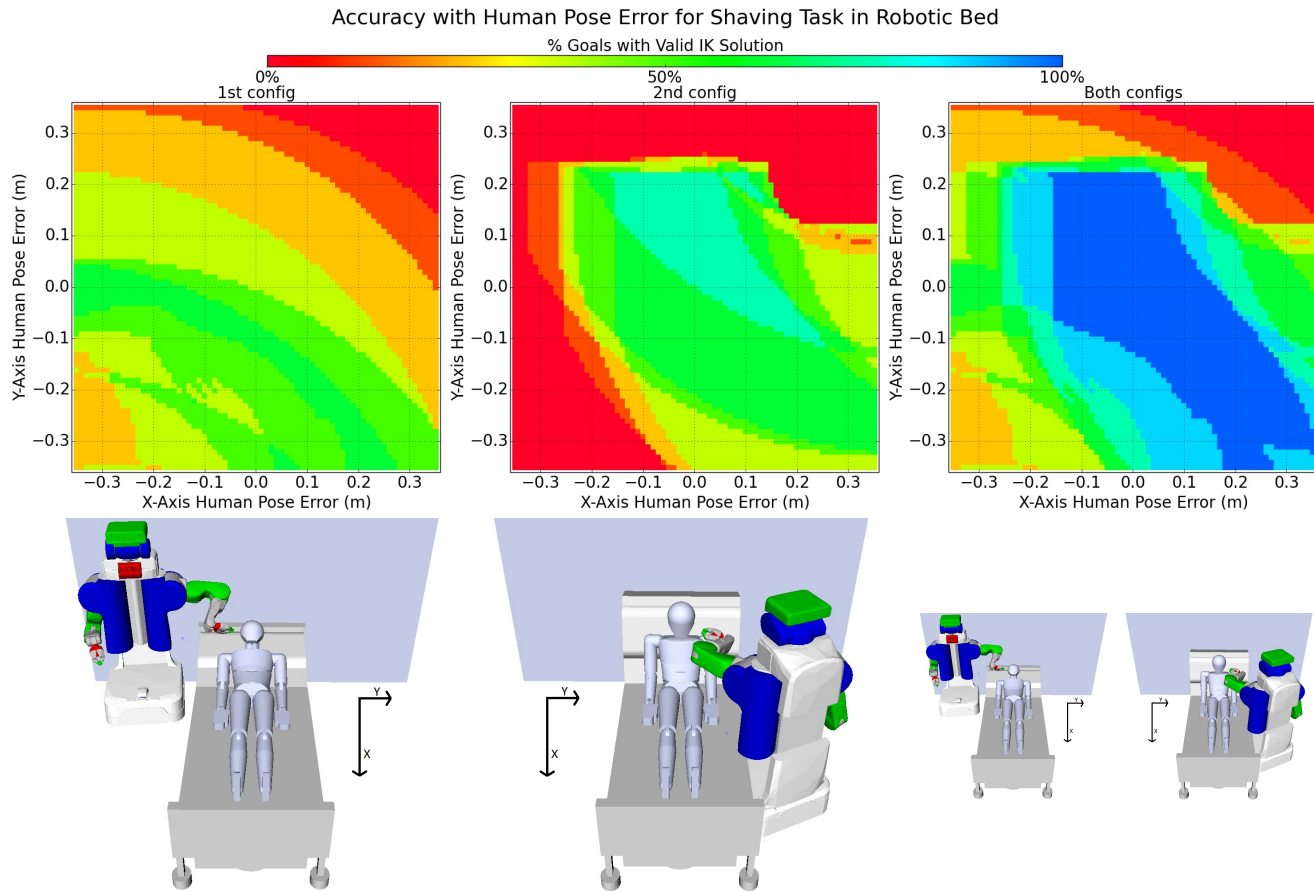


Fig. 10: Visualization of the robustness of TOC's selected configurations for the shaving task in the robotic bed. (Top) Percentage of goals reached from the first, second, and both configurations for error in 1cm increments in the x-y position of the person. (bottom) The first and second configurations of the PR2, and the two configurations combined on the right. Color is necessary to interpret this figure. The blue region represents when all goals can be reached.

with their TOC score. Figure 13 shows the results of the analysis. Higher TOC score is correlated with accuracy and inversely correlated with variance in accuracy.

5 Discussion

We have shown results with a single type and source of error. However, we expect TOC to be able to deal with many types and sources of error. If we knew all sources of error apriori, we could explicitly model them, to improve selection of robot configurations. Such a method would be similar to those from Hsu et al (1999) and Stulp et al (2009), described in Section 2.2. It should be noted, however, that movement of the person (e.g., pose estimation error) does not directly translate into motion of the robot's base, so directly using these evaluations as part of a method to select the robot's configuration can be difficult. Our results provide evidence that TOC can often select robot configurations that are more robust to error in the person's pose than baseline methods.

This is seen in many of the tasks and environments we examined, but is most pronounced in more challenging tasks that may need more than a single robot configuration to complete.

We observed that baseline methods work well for many tasks and they selected configurations, on average, faster than TOC. For its offline computations, TOC took on average 70 minutes for each task running in a single thread on a 64-bit, 14.04 Ubuntu operating system with 8 GB of RAM and a 3.40 GHz Intel Core i7-3770 CPU. The IK solver baseline we implemented runs faster, on average 6 minutes and often less than 1 minute for each task. These results suggest that this baseline may work well for many tasks that only require a single robot configuration and where there is little error between model and reality. The capability map with collision detection also performed well on many tasks and took on average 34 minutes to select a configuration. Note that this is the time to run these algorithms either offline within our framework or online. As in assistive robotics, in many robotics applications the speed of online selection is important and 6 minutes, 34

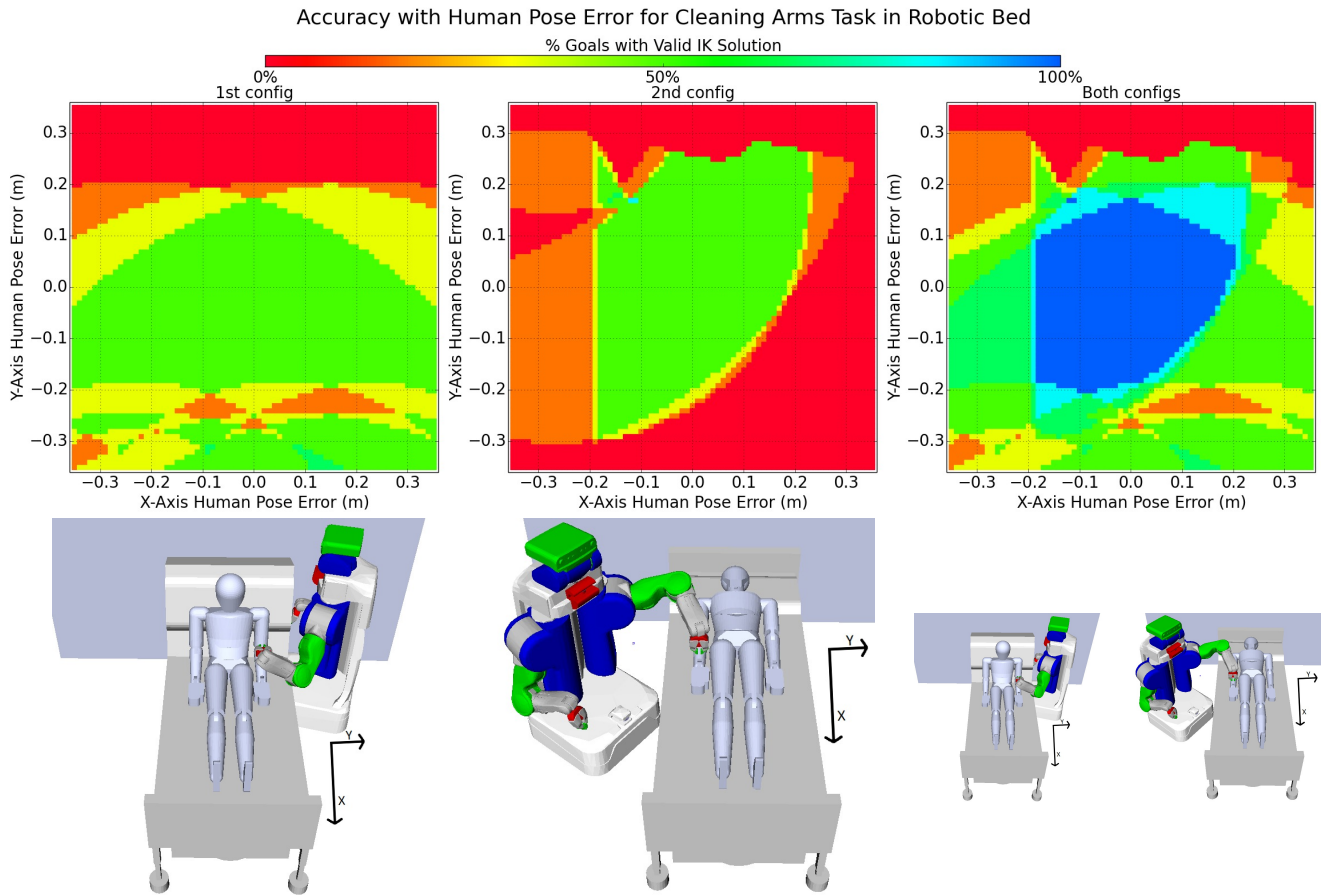


Fig. 11: Visualization of the robustness of TOC’s selected configurations for the arm cleaning task in the robotic bed. (Top) Percentage of goals reached from the first, second, and both configurations for error in 1cm increments in the x-y position of the person. (bottom) The first and second configurations of the PR2, and the two configurations combined on the right. Color is necessary to interpret this figure. The blue region represents when all goals can be reached.

minutes, and 70 minutes are all too long for a user to wait for a robot to decide where to move. Additionally, there may be specifically important or common tasks that take place in environments that are known beforehand. In this case, it can be valuable to take additional time offline to find solutions, using our framework, to take advantage of prior knowledge and speed up the responsiveness of the online process.

We sought to handle fairly the comparison between TOC and baseline methods by using the same sampling for each. However, because of the nature of the search problem, using other search methods, additional heuristics, or other meta-parameters for the search (e.g., different population size) may find better configurations than those found in our evaluations.

We observed a trade-off when selecting robot configurations. In general, moving the PR2 closer tends to improve the arm’s dexterity, but tends to make collisions more likely. An assumption in this work is that contact is bad and should be avoided. However, Grice et al (2013) found that contact can be both beneficial and acceptable during robotic assistance.

Allowing contact can increase the space of reachable poses, and there are methods for controlling contact safely (Killpack et al, 2016).

5.1 Design Application

TOC may also be used to assist in the design of environments. For example, in our evaluations with the robotic bed, TOC selected a configuration for the bed by including the bed’s DoF in the robot configuration. TOC could similarly optimize many other continuous controllable parameters of the environment. Comparison of TOC scores between a robotic bed and a standard, static bed may demonstrate the value added by a robotic bed. By recognizing that for some tasks a lower bed height improves performance and for other tasks a higher bed height improves performance, we may recognize that an adjustable bed may be preferable to allow the bed to reconfigure to the desired height for each task. As detailed in Section 3.5, TOC can be used to assist in design for param-

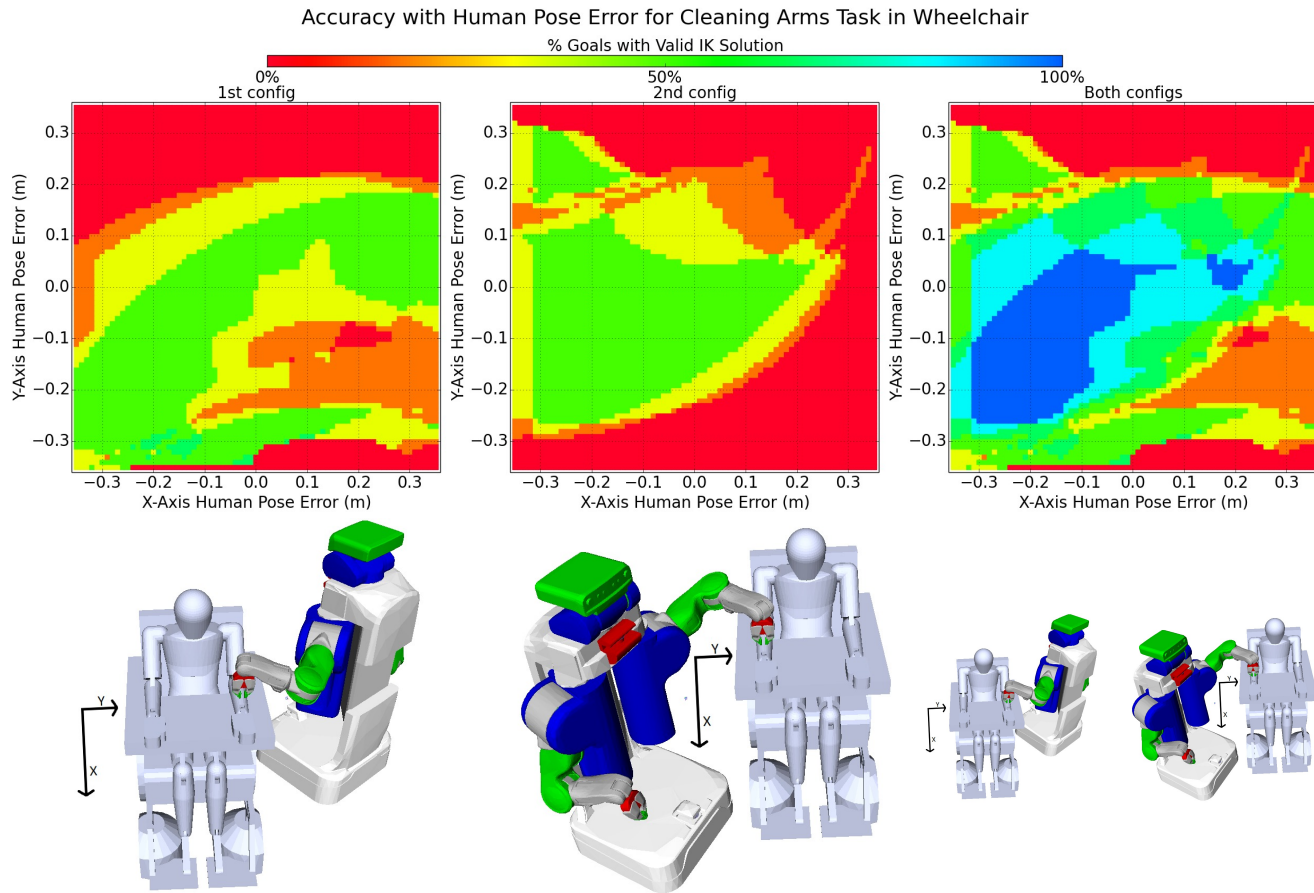


Fig. 12: Visualization of the robustness of TOC's selected configurations for the arm cleaning task in the wheelchair. (Top) Percentage of goals reached from the first, second, and both configurations for error in 1cm increments in the x-y position of the person. (bottom) The first and second configurations of the PR2, and the two configurations combined on the right. Color is necessary to interpret this figure. The blue region represents when all goals can be reached.

ters with discrete choices by including it as an uncontrollable parameter in the optimization. In this way, you might decide to put the bed against the wall, 0.5 m away from the wall, or 1 m away from the wall. For example, we have found that for the shaving task, if there is sufficient space behind the bed, the PR2 can perform the task from a single configuration instead of requiring two configurations. Figure 14 shows the configuration found by TOC for shaving in the robotic bed without a wall and visualizes the robustness to error in the pose of the person.

5.2 Limitations

There are some limitations to our work with TOC and our evaluation. Although the framework of TOC allows it to search for sets of robot configurations of cardinality larger than 2, we limited it to two in our evaluation. We made this choice because we found that more than two robot configurations were not needed for any of the tasks examined.

We hand designed the task models for our evaluation in simulation, but have not investigated how well the task models actually represent the tasks. In addition, all tasks in this work were defined with full 6-DoF goal poses, although some tasks, such as sponge baths, have position requirements and few orientation requirements. We also did not address tasks with complex motions in which the trajectory between goals poses is important, such as dressing, or tasks with high strength requirements, such as lifting or ambulating.

Joint-limit-weighted kinematic isotropy, the foundation of our TC-manipulability score, does not account for environmental constraints. There may be value in preferring joint configurations away from obstacles. We have mitigated the risk of collisions using a safety margin on the environment and user models at the cost of decreasing the valid search space and eliminating valid solutions. Explicitly penalizing proximity to collisions in the objective function, as was done by Vahrenkamp et al (2012), may be another way to mitigate this issue at the cost of additional computation time.

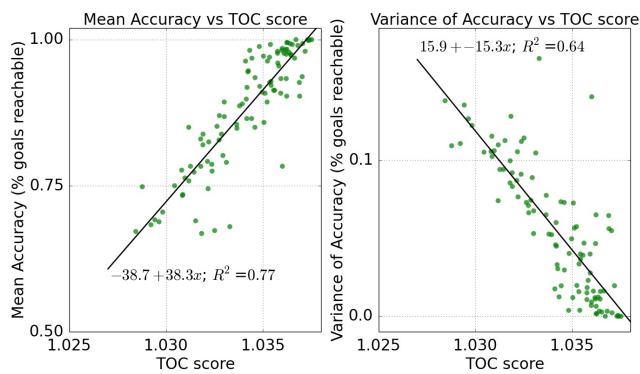


Fig. 13: Increasing TOC score is correlated to accuracy and inversely correlated to variance in accuracy. TOC score above 1.0 means a collision-free IK solution exists to all goals. The amount above 1.0 is the weighted TC-manipulability score for the configuration.

TOC also does not determine if there are valid paths to reach collision-free IK solutions, which may be problematic when there are environmental constraints. A motion planner could be used to check for valid paths at the cost of computation time. Although computation time is often a less critical concern for offline processes, it must remain reasonable. We elected to ignore proximity to collisions and the question of the existence of valid paths to achieve lower computation time.

6 Conclusion

In this work, we have presented task-centric optimization of robot configurations (TOC), a method to select one or more configurations for robots to assist with tasks around a person's body. TOC uses TC-reachability and TC-manipulability, metrics that we have developed, to represent the robot's dexterity, and implicitly handle error. TOC is particularly suitable for assistive tasks, where there are a set of desired tasks known a priori that can be modeled as a set of end effector poses with respect to relevant reference frames. We have shown that TOC can determine a set of one or two robot configurations from which the robot can perform a task well. TOC performs the bulk of its computation offline using models of the task, robot, environment, and person to generate a function that rapidly (≤ 1 second) estimates the optimal set of robot configurations for a task given observations at runtime. We provide evidence that configurations selected by TOC are robust to state estimation errors between the models used offline and observations at runtime. We created 9 models of assistive tasks to test our system in simulation and showed that for each task TOC's average success rate was higher than or comparable to three baseline algorithms from literature. TOC had an overall average success rate of

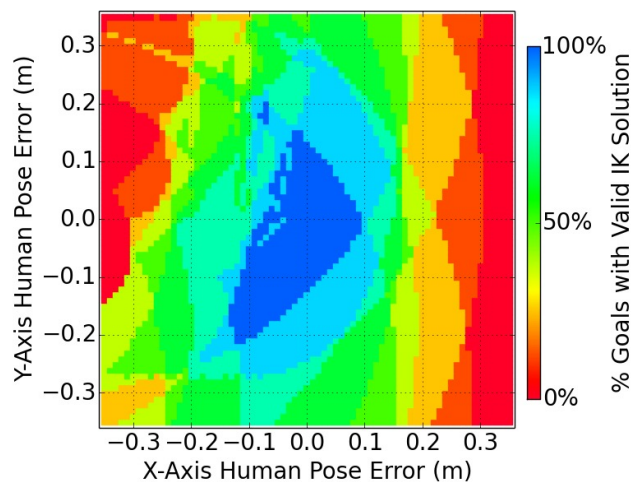
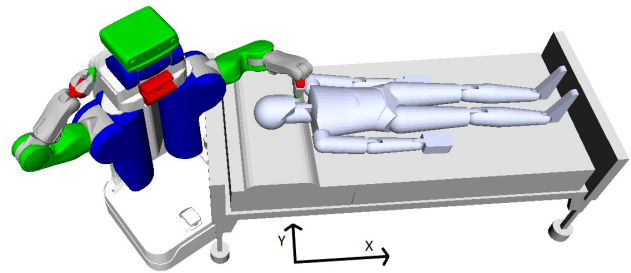


Fig. 14: The PR2 can perform the shaving task on the person in bed from a single location if there is no wall behind the bed. (Top) the configuration TOC selected (bottom) a visualization of the robustness to error in the person's pose on the bed for this configuration.

90.6% compared to 50.4%, 43.5%, and 58.9% for baseline methods.

References

- (2015) Canadian Partnership for Stroke Recovery. "Stroke Engine". URL <http://www.strokengine.ca/>, accessed: 2018-01-01
- (2017) The Wright Stuff, Inc. "The Wright Stuff healthcare products that make life easier". URL <https://www.thewrightstuff.com/>, accessed: 2018-01-01
- Andersen CK, Wittrup-Jensen KU, Lolk A, Andersen K, Kragh-Sørensen P (2004) Ability to perform activities of daily living is the main factor affecting quality of life in patients with dementia. *Health and quality of life outcomes* 2(1):52
- Beeson P, Ames B (2015) Trac-ik: An open-source library for improved solving of generic inverse kinematics. In:

- Humanoid Robots (Humanoids), 2015 IEEE-RAS 15th International Conference on, IEEE, pp 928–935
- Bien Z, Chung MJ, Chang PH, Kwon DS, Kim DJ, Han JS, Kim JH, Kim DH, Park HS, Kang SH, et al (2004) Integration of a rehabilitation robotic system (kares ii) with human-friendly man-machine interaction units. *Autonomous robots* 16(2):165–191
- Burget F, Bennewitz M (2015) Stance selection for humanoid grasping tasks by inverse reachability maps. In: *Robotics and Automation (ICRA)*, 2015 IEEE International Conference on, IEEE, pp 5669–5674
- Chan TF, Dubey RV (1995) A weighted least-norm solution based scheme for avoiding joint limits for redundant joint manipulators. *IEEE Transactions on Robotics and Automation* 11(2):286–292
- Chen TL, Ciocarlie M, Cousins S, et al (2013) Robots for humanity: A case study in assistive mobile manipulation
- Dario P, Guglielmelli E, Laschi C, Teti G (1999) Movaid: a personal robot in everyday life of disabled and elderly people. *Technology and Disability* 10(2):77–93
- Diankov R (2010) Automated construction of robotic manipulation programs
- Diankov R, Kuffner J (2008) Openrave: A planning architecture for autonomous robotics. Robotics Institute, Pittsburgh, PA, Tech Rep CMU-RI-TR-08-34 79
- Diankov R, Ratliff N, Ferguson D, Srinivasa S, Kuffner J (2008) Bispaces planning: Concurrent multi-space exploration. *Proceedings of Robotics: Science and Systems IV* 63
- Dong J, Trinkle JC (2015) Orientation-based reachability map for robot base placement. In: *Intelligent Robots and Systems (IROS)*, 2015 IEEE/RSJ International Conference on, IEEE, pp 1488–1493
- Elbanhawi M, Simic M (2014) Sampling-based robot motion planning: A review. *IEEE Access* 2:56–77
- Garrett CR, Lozano-Pérez T, Kaelbling LP (2015) Backward-forward search for manipulation planning. In: *Intelligent Robots and Systems (IROS)*, 2015 IEEE/RSJ International Conference on, IEEE, pp 6366–6373
- Gienger M, Janssen H, Goerick C (2005) Task-oriented whole body motion for humanoid robots. In: *Humanoid Robots*, 2005 5th IEEE-RAS International Conference on, IEEE, pp 238–244
- Goodin HJ (2003) The nursing shortage in the United States of America: an integrative review of the literature. *J Adv Nurs*
- Graf B, Reiser U, Hägele M, Mauz K, Klein P (2009) Robotic home assistant care-o-bot® 3-product vision and innovation platform. In: *Advanced Robotics and its Social Impacts (ARSO)*, 2009 IEEE Workshop on, IEEE, pp 139–144
- Grey MX, Garrett CR, Liu CK, Ames AD, Thomaz AL (2016) Humanoid manipulation planning using backward-forward search. In: *Intelligent Robots and Systems (IROS)*, 2016 IEEE/RSJ International Conference on, IEEE, pp 5467–5473
- Grice P, Kemp CC (2016) Assistive mobile manipulation: Designing for operators with motor impairments. In: *Proceedings of Robotics: Science and Systems (RSS 2016) Workshop on Socially and Physically Assistive Robotics for Humanity*,
- Grice P, Chitalia Y, Rich M, et al (2016) Autobod: Open hardware for accessible web-based control of an electric bed. RESNA
- Grice PM, Killpack MD, Jain A, Vaish S, Hawke J, Kemp CC (2013) Whole-arm tactile sensing for beneficial and acceptable contact during robotic assistance. In: *Rehabilitation Robotics (ICORR)*, 2013 IEEE International Conference on, IEEE, pp 1–8
- Hammond F, Shimada K (2011) Multi-objective weighted isotropy measures for the morphological design optimisation of kinematically redundant manipulators. *International Journal of Mechatronics and Manufacturing Systems* 4(2):150–170
- Hammond III FL, Shimada K (2009) Improvement of kinematically redundant manipulator design and placement using torque-weighted isotropy measures. In: *Advanced Robotics*, 2009. ICAR 2009. International Conference on, IEEE, pp 1–8
- Hawkins KP, Grice PM, Chen TL, et al (2014) Assistive mobile manipulation for self-care tasks around the head. In: *Computational Intelligence in Robotic Rehabilitation and Assistive Technologies (CIR2AT)*, 2014 IEEE Symposium on, IEEE, pp 16–25
- Hsu D, Latcombe JC, Sorkin S (1999) Placing a robot manipulator amid obstacles for optimized execution. In: *Assembly and Task Planning, 1999. (ISATP'99) Proceedings of the 1999 IEEE International Symposium on*, IEEE, pp 280–285
- Institute of Medicine (2008) *Retooling for an Aging America: Building the Health Care Workforce*. The National Academies Press
- Jain A, Kemp CC (2010) El-e: an assistive mobile manipulator that autonomously fetches objects from flat surfaces. *Autonomous Robots* 28(1):45–64
- Kapusta A, Kemp CC (2016) Optimization of robot configurations for assistive tasks. In: *Proceedings of Robotics: Science and Systems (RSS 2016) Workshop on Planning for Human-Robot Interaction: Shared Autonomy and Collaborative Robotics*
- Kapusta A, Park D, Kemp CC (2015) Task-centric selection of robot and environment initial configurations for assistive tasks. In: *Intelligent Robots and Systems (IROS)*, 2015 IEEE/RSJ International Conference on, IEEE, pp 1480–1487

- Kapusta A, Chitalia Y, Park D, Kemp CC (2016) Collaboration between a robotic bed and a mobile manipulator may improve physical assistance for people with disabilities
- Killpack MD, Kapusta A, Kemp CC (2016) Model predictive control for fast reaching in clutter. *Autonomous Robots* 40(3):537–560
- Kim JO, Khosla K (1991) Dexterity measures for design and control of manipulators. In: *Intelligent Robots and Systems '91. Intelligence for Mechanical Systems, Proceedings IROS'91. IEEE/RSJ International Workshop on, IEEE*, pp 758–763
- Klein CA, Blaho BE (1987) Dexterity measures for the design and control of kinematically redundant manipulators. *The International Journal of Robotics Research* 6(2):72–83
- Kruse T, Pandey AK, Alami R, Kirsch A (2013) Human-aware robot navigation: A survey. *Robotics and Autonomous Systems* 61(12):1726–1743
- Kumar S, Sukavanam N, Balasubramanian R (2010) An optimization approach to solve the inverse kinematics of redundant manipulator. *International Journal of Information and System Sciences (Institute for Scientific Computing and Information)* 6(4):414–423
- Lee J (1997) A study on the manipulability measures for robot manipulators. In: *Intelligent Robots and Systems, 1997. IROS'97., Proceedings of the 1997 IEEE/RSJ International Conference on, IEEE*, vol 3, pp 1458–1465
- Leidner D, Dietrich A, Schmidt F, Borst C, Albu-Schaffer A (2014) Object-centered hybrid reasoning for whole-body mobile manipulation. In: *Robotics and Automation (ICRA), 2014 IEEE International Conference on, IEEE*, pp 1828–1835
- Lindemann SR, LaValle SM (2005) Current issues in sampling-based motion planning. *Robotics Research* pp 36–54
- Mainprice J, Sisbot EA, Jaillet L, Cortes J, Alami R, Simeon T (2011) Planning human-aware motions using a sampling-based costmap planner. In: *Robotics and Automation (ICRA), 2011 IEEE International Conference on, IEEE*, pp 5012–5017
- Mumm J, Mutlu B (2011) Human-robot proxemics: physical and psychological distancing in human-robot interaction. In: *Proceedings of the 6th international conference on Human-robot interaction, ACM*, pp 331–338
- Porges O, Stouraitis T, Borst C, Roa MA (2014) Reachability and capability analysis for manipulation tasks. In: *ROBOT2013: First Iberian Robotics Conference, Springer*, pp 703–718
- Schaeffer C, May T (1999) Care-o-bot-a system for assisting elderly or disabled persons in home environments. *Assistive technology on the threshold of the new millenium*
- Sisbot EA, Marin LF, Alami R, Simeon T (2006) A mobile robot that performs human acceptable motions. In: *Intelligent Robots and Systems, 2006 IEEE/RSJ International Conference on, IEEE*, pp 1811–1816
- Sisbot EA, Marin-Urias LF, Alami R, Simeon T (2007) A human aware mobile robot motion planner. *Robotics, IEEE Transactions on* 23(5):874–883
- Sisbot EA, Marin-Urias LF, Broquere X, Sidobre D, Alami R (2010) Synthesizing robot motions adapted to human presence. *International Journal of Social Robotics* 2(3):329–343
- Smits R (2006) KDL: Kinematics and Dynamics Library. URL <http://www.orocos.org/kdl>, accessed: 2018-01-01
- Spong MW, Hutchinson S, Vidyasagar M (2006) *Robot modeling and control*, vol 3. Wiley New York
- Stilman M, Kuffner JJ (2005) Navigation among movable obstacles: Real-time reasoning in complex environments. *International Journal of Humanoid Robotics* 2(04):479–503
- Stocco L, Salcudean S, Sassani F (1998) Matrix normalization for optimal robot design. In: *Robotics and Automation, 1998. Proceedings. 1998 IEEE International Conference on, IEEE*, vol 2, pp 1346–1351
- Stulp F, Fedrizzi A, Beetz M (2009) Learning and performing place-based mobile manipulation. In: *Development and Learning, 2009. ICDL 2009. IEEE 8th International Conference on, IEEE*, pp 1–7
- Takayama L, Pantofaru C (2009) Influences on proxemic behaviors in human-robot interaction. In: *Intelligent Robots and Systems, 2009. IROS 2009. IEEE/RSJ International Conference on, IEEE*, pp 5495–5502
- Tan J, Gu Y, Turk G, Liu CK (2011) Articulated swimming creatures. In: *ACM Transactions on Graphics (TOG), ACM*, vol 30, p 58
- Tilley AR (2002) *The Measure of Man and Woman: Human Factors in Design*. Wiley, New York
- Topping M (1999) The development of handy 1. a robotic system to assist the severely disabled. In: *Int. Conf. Rehab. Robo.*, pp 244–249
- Topping M, Smith J (1998) The development of Handy 1, a rehabilitation robotic system to assist the severely disabled. *Industrial Robot* 25(5):316–20
- Tsai MJ (1986) *Workspace geometric characterization and manipulability of industrial robots*. PhD thesis, The Ohio State University
- Vahrenkamp N, Asfour T, Metta G, Sandini G, Dillmann R (2012) Manipulability analysis. In: *Humanoid Robots (Humanoids), 2012 12th IEEE-RAS International Conference on, IEEE*, pp 568–573
- Vahrenkamp N, Asfour T, Dillmann R (2013) Robot placement based on reachability inversion. In: *Robotics and Automation (ICRA), 2013 IEEE International Conference on, IEEE*, pp 1970–1975
- Vest M, Murphy T, Araujo K, Pisani M, et al (2011) Disability in activities of daily living, depression, and quality of life

among older medical ICU survivors: a prospective cohort study

- Walters ML, Dautenhahn K, Te Boekhorst R, Koay KL, Kaouri C, Woods S, Nehaniv C, Lee D, Werry I (2005) The influence of subjects personality traits on personal spatial zones in a human-robot interaction experiment. In: Robot and Human Interactive Communication, 2005. ROMAN 2005. IEEE International Workshop on, IEEE, pp 347–352
- Walters ML, Dautenhahn K, Te Boekhorst R, Koay KL, Syrdal DS, Nehaniv CL (2009) An empirical framework for human-robot proxemics. *Procs of New Frontiers in Human-Robot Interaction*
- Walters ML, Oskoei MA, Syrdal DS, Dautenhahn K (2011) A long-term human-robot proxemic study. In: RO-MAN, 2011 IEEE, IEEE, pp 137–142
- Wiener JM, Hanley RJ, Clark R, Nostrand JFV (1990) Measuring the activities of daily living: Comparisons across national surveys. *Journal of Gerontology: SOCIAL SCIENCES* 45(6):S229–237
- Yoshikawa T (1984) Analysis and control of robot manipulators with redundancy. In: *Robotics research: the first international symposium*, Mit Press Cambridge, MA, USA, pp 735–747
- Zacharias F, Borst C, Hirzinger G (2007) Capturing robot workspace structure: representing robot capabilities. In: *Intelligent Robots and Systems, 2007. IROS 2007. IEEE/RSJ International Conference on, Ieee*, pp 3229–3236
- Zacharias F, Sepp W, Borst C, Hirzinger G (2009) Using a model of the reachable workspace to position mobile manipulators for 3-d trajectories. In: *Humanoid Robots, 2009. Humanoids 2009. 9th IEEE-RAS International Conference on, IEEE*, pp 55–61